TÜBİTAK

Turkish Journal of Chemistry

http://journals.tubitak.gov.tr/chem/

Research Article

Turk J Chem
(2013) 37: 547 – 557

doi:10.3906/kim-1302-17

DFT study of tautomerism in aklavinone

Burhan Lemi TÜRKER*
Department of Chemistry, Faculty of Arts and Sciences, Middle East Technical University, Ankara, Turkey

Received: 11.02.2013 • **Accepted:** 24.04.2013 • **Published Online:** 12.07.2013 • **Printed:** 05.08.2013

Abstract: Aklavinone has an anthraquinone-based chromophore and its backbone highly resembles the kernel of some anthracycline antibiotics that possess anticancer activity, e.g., daunomycin. Since aklavinone's structure possesses many –OH groups and 2 keto groups, it is quite probable that certain tautomeric equilibria may occur. Presently, aklavinone prototropic tautomers possessing embedded anthraquinone moiety have been investigated quantum chemically by using density functional theory at the levels of RB3LYP/6-31G(d) and RB3LYP/6-31G(d,p). Additionally, IR spectra of the tautomers were calculated. Moreover, the phenolate ions obtained from the most stable tautomer in water were considered, and the protonation of this tautomer at various possible sites was investigated quantum chemically.

Key words: Aklavinone, tautomerism, anthracycline, daunomycin, DFT calculations

1. Introduction

Anthracyclines are a group of glycosides, most of which exhibit antibiotic action. They are produced in nature by various *Streptomyces* species.[1] One of them is the cancer chemotherapy medicine daunomycin.[2] *Streptomyces* species act as sources of anthraquinones, which are quinones having 4 rings. Quinones are compounds having a fully conjugated cyclic dione structure. They commonly occur as the constituents of biologically relevant molecules. Marine *Streptomyces* are an especially rich source of biologically active quinones.[3] Aklavinone exists in extracts of many *Streptomyces* species; one of them is the strain MST-77755.[1]

Aklavinone (**1**) exists as the parent aglycons of 2 families of glycosidically derived anthracycline antibiotics that possess significant anticancer activity.[4,5] The skeleton of the chromophore system of aklavinone is present in great extent in the chromophoric moiety of daunomycin, which is a well-known anticancer agent. The structure of aklavinone has many –OH groups of which 2 are phenolic and the other 2 are carbinol OH groups. Aklavinone also possesses 2 keto groups. Because of the possibility of tautomerism, the number of these groups varies from one tautomer to other (see Figure 1). In the structure of daunomycin, the phenolic –OH groups of aklavinone are in methyl ether form. Additionally, their alicyclic rings (daunomycin and aklavinone) possess different substituents.

Oki et al. have reported on the isolation, characterization, and biological activity of 7 antibiotics, including aklavinone.[6,7] Of these antibiotics, aclacinomycin-A was investigated substantially and found to possess high anticancer activity. Additionally it was demonstrated to be less toxic than the clinically useful agents rhodomycin and daunorubicin.[6–10]

*Correspondence: lturker@metu.edu.tr
Dedicated to the memory of Professor Ayhan S. Demir

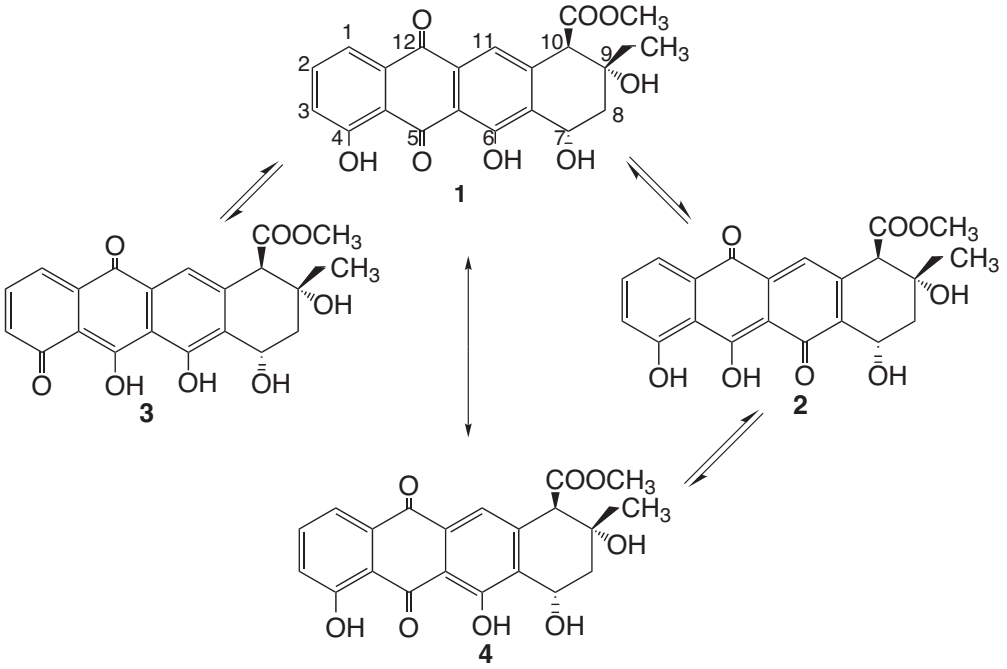

Figure 1. Tautomers presently considered and numbering of carbons in aklavinone.

Its biological importance forced chemists to investigate the total synthesis of this aklavinone-like chemical.[11–14] Electron-deficient o-quinoid pyrones were employed by Jones and Lock for the synthesis of aklavinone.[15] Some researchers obtained certain aklavinone derivatives with the reduction of daunomycin and 7-deoxydaunomycin.[16] On the other hand, Kodoma et al. reported an electron spin resonance study on quinone-containing carcinostatics, aclocinomycin-A, and its derivatives.[17] In their study, the hyperfine structure of ESR spectra was satisfactorily reproduced by certain simulations, using the hyperfine coupling constants obtained by semiempirical INDO molecular orbital method.[17]

Furthermore, isotopic labeling experiments have shown that a tetra cyclic precursor has been used in daunomycin synthesis in *Streptomyces galilaeus*, whereas aklavinone in turn is synthesized from acetate.[18] Aklavinone is commonly found in *Streptomyces* species even in some living in marine environments.[1,3]

Daunomycin, which contains an aklavinone-type kernel (basically 11-hydroxyaklavinone backbone), has been long known to possess an effective antitumor action. Tautomerism in 7-deoxyalklavinone has been mentioned in the literature.[19] The theoretical treatment of tautomerism in 11-hydroxyaklavinone has also appeared in the literature recently.[20] It has been shown that the mechanism of the biological effect of daunomycin is due to its ability to set itself between pairs of DNA bases.[21] The responsible part is the chromophore of daunomycin (aklavinone-like moiety), which separates DNA pairs to find its place between them, interacting with various hydrogen bond forming sites.[21] Therefore, tautomerism studies in these systems are highly important in terms of medicinal mechanism of action as well as being interesting in the pure chemical sense.

The type of breaking and forming of chemical bonds divides reactions into 2 categories, namely homolytic and heterolytic (radical and ionic, respectively). It may be postulated that tautomeric conversions of both types must exist. However, to date, mostly heterolytic (cationotropic and anionotropic) tautomeric conversions have been studied.[22]

Quantum chemical investigation of aklavinone, which has various –OH groups and 2 keto groups of

quinoid type (which is capable of exhibiting many tautomeric forms), may shed some light on the prototropic equilibria that might occur in daunomycin and similar compounds from *Streptomyces* species. Presently, some prototropic tautomers of aklavinone have been investigated quantum chemically (within the realm of density functional theory (DFT)). Then the phenolate ions and the protonated forms of the most stable tautomer of aklavinone in water have been subjected to quantum chemical investigation.

2. Results and discussion

2.1. Structures

Figure 1 shows the structure and numbering of aklavinone. As seen, it contains 2 phenolic as well as 2 alcoholic –OH groups in addition to the keto groups. The chromophoric part of it can be treated as trihydroxy anthraquinone moiety. The structure possesses the phenolic –OH groups in such positions that they enable one to write down various tautomeric forms; meanwhile, the aromatic nature of some of the phenolic rings is lost. However, in some forms of the prototropic tautomers, 1 or 2 aromatic sextet(s) is/are retained. Various prototropic tautomers of aklavinone (**1**) that are interconvertible via 1,5-type tautomeric routes are depicted in Figure 1. At first sight, structure **2** can be considered as 1,5-tautomer of **1** based on structure **4**. However, **1** and **4** are resonance structures. In tautomers **2** and **3** a single phenolic ring occurs, whereas in **1** and **4** the skeletons contain 1,4-anthraquinone moiety having 2 phenolic –OH groups. In aklavinone (**1** or **4**) the 2 aromatic sextets are isolated Clar's sextets.

The stabilities of these tautomers (**1**–**3**), are worth considering theoretically. The stabilities of the presently considered tautomers seem to be affected by intramolecular hydrogen bonding. Figure 2 shows the geometry optimized structures (some bond lengths are displayed too) of aklavinone and its tautomers presently considered. As seen in the figure, in structures **2** and **3** hydrogen bonding is clearly seen between the –OH group(s) and the keto or -OH group(s) next to it. The conformation of the ester methoxy group on the alicyclic ring is different in **2** from those in **1** and **3**. Moreover, the conformation of the ethyl group located at position 9 (see Figure 1 for the position) varies from one tautomer to the other, which is indicative of how the tautomeric changes influence the conformation of such a distant group.

2.2. Stabilities

Table 1 shows the total electronic energies of the species considered. In vacuum conditions the stability order is found to be **2** > **3** > **1** (RB3LYP/6-31G(d,p)). Although tautomer **2** contains an enolic group, it is more stable than the others in vacuum. The calculations also have indicated that this order is somewhat changed in aqueous medium, that is **1** > **2** > **3** (see Table 2). In vacuum (the first series) **1** appears to be the least stable structure even though it contains 2 aromatic sextets in its structure. Structure **2** is more stable than the others in vacuum. Compared to **1** it has one less Clar's sextet but possesses an extended conjugation. It has a smaller $\Delta\varepsilon$ value (see the following section for the LUMO–HOMO energy gap). When one compares the stability orders in the vacuum and aqueous conditions, the effect of solvation/hydrogen bonding appears to be not negligible and it affects the stability order of the tautomers considered. Many examples exist in the literature reflecting the importance of solvents on the tautomeric equilibria. One of them is the 9-anthrone/9-anthranol equilibrium (related to the aklavinone case), where the equilibrium lies predominantly on the side of the keto form in the gas phase and inert solvents, whereas in contrast the enol form is favored in protic solvents.[23] This observation at first sight seems to be quite contradictory to the results of the present calculations (enol forms **2** and **3** are more stable in vacuum but less stable in water than **1**). Note that in structures **1**–**3** the total numbers of enolic

(some phenolic) and keto groups are the same. Therefore, the stabilities of these tautomers are dictated by their topologies, which in general influence the intra- and intermolecular hydrogen bonding, charge–dipole and dipole–dipole interactions, etc. Moreover, local dipole–dipole interactions may contribute to the whole stability

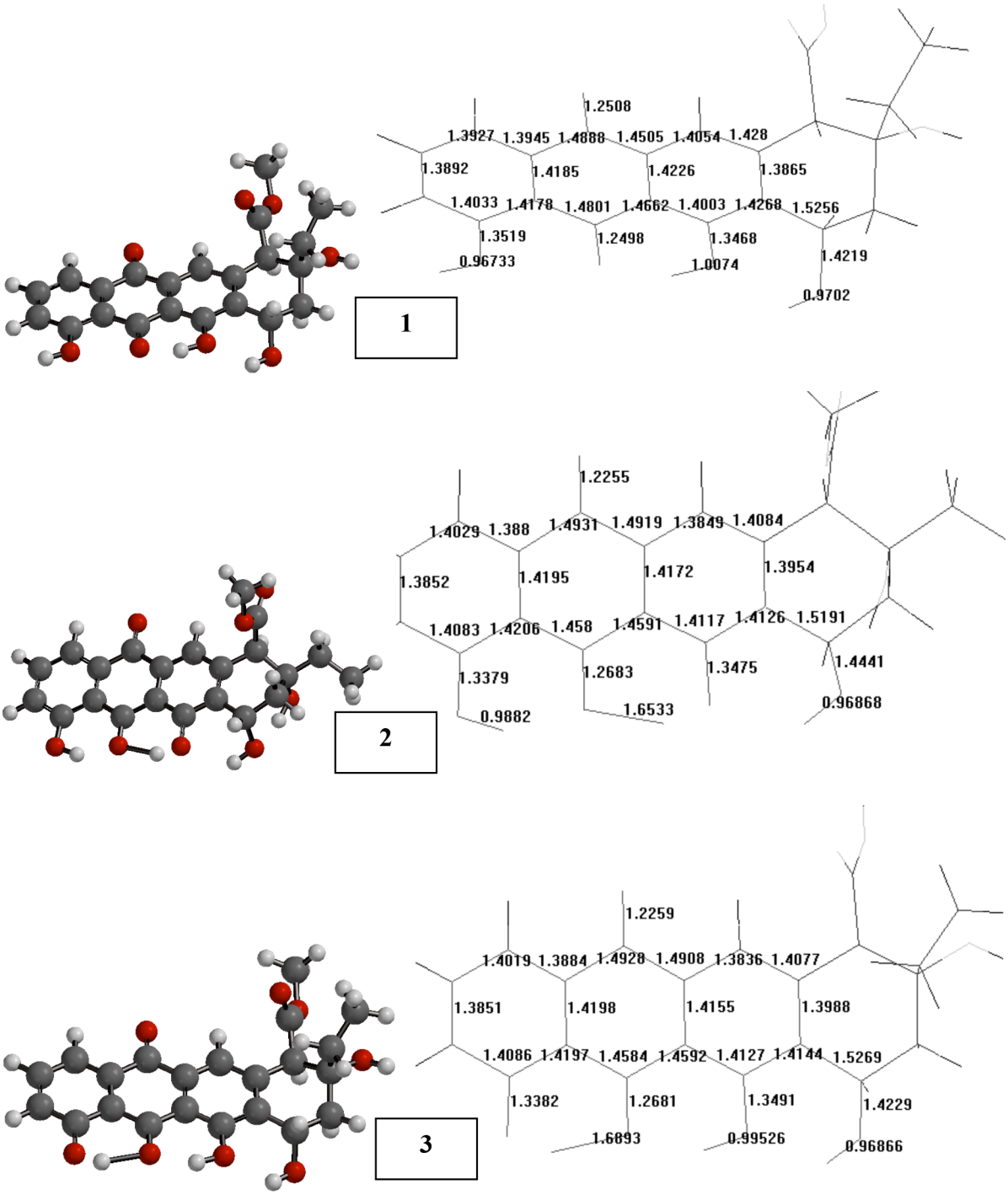

Figure 2. The geometry optimized structures and some bond lengths (Å) of the tautomers considered (RB3LYP/6-31G(d,p)).

of each tautomer. The intramolecular hydrogen bondings in **2** and **3** are responsible for their better stability (in vacuum) over **1**, whereas in aqueous conditions intermolecular hydrogen bondings and some other factors should reverse the order. The RB3LYP/6-31G(d) type (a lower level treatment) calculations also produce the same stability order (in vacuum) as **2** > **3** > **1** and in aqueous conditions as **1** > **2** > **3**.

Table 1. Total energy (kJ) values of the structures considered (RB3LYP/6-31G(d,p)).

Structure	Total energy	Corrected total energy
1	–3,812,867.77	–3,811,843.81
2	–3,812,972.79	–3,811,922.58
3	–3,812,920.28	–3,811,896.32

Table 2. Total energy (kJ) values of the structures considered in aqueous medium. RB3LYP/6-31G(d,p).

Structure	Total energy	Corrected total energy
1	–3,813,077.81	–3,812,053.86
2	–3,813,025.30	–3,811,975.09
3	–3,812,999.04	–3,811,975.09

Table 3 displays the standard free energy of formation values calculated at the level of B3LYP/6-31G(d,p) (pseudopotential). The order from the lowest (the most negative G^0 value) to the highest is **2** < **3** < **1**, which is the order of total energies in the vacuum conditions. The order indicates clearly the fact that **2** is the most favorable in terms of the free energy of formation criterion.

Table 3. G° and relative G° (kJ/mol) values of the structures considered. (RB3LYP/6-31G(d,p)).

Structure	G° (kJ/mol)	Rel G° (kJ/mol)
1	–3,811,951	91.99
2	–3,812,043	0
3	–3,812,014	29.93

The free energy of the tautomeric change between any 2 tautomeric forms can be calculated by using the data in Table 3. The results of thermodynamic calculations have indicated that the most favorable conversion of **1** is **1**→**3** (63 kJ/mol), followed by **1**→**2** (92 kJ/mol).

2.3. Spectra

Figure 3 shows the calculated (B3LYP/6-31G(d,p)) IR spectra of some selected tautomers (harmonic frequencies). The alcoholic and phenolic –OH stretchings occur above 3250 cm^{-1}, whereas the saturated and unsaturated C=O stretchings happen in the region of 1800–1600 cm^{-1}, having varying strengths. Note that the values obtained from the calculated spectra are to be dealt with on a relative basis.

Table 4 shows the HOMO, LUMO, and interfrontier molecular orbital energy gap ($\Delta\varepsilon$) values of the species of concern (DFT treatment). Tautomer **2** is characterized by the lowest lying HOMO energy value. The order is **2** < **3** < **1.** The order of LUMO energies is the same. As for the $\Delta\varepsilon$ values, **1** has the largest energy gap while **2** possesses the smallest one (**1** > **3** > **2**). The reason for the smallest $\Delta\varepsilon$ value of **2** is the extended conjugation present in its structure. Thus the tautomerism in the series should cause a red shift compared to aklavinone. The frontier energies (HOMO and LUMO) and the interfrontier energy gaps given in Table 4 are of

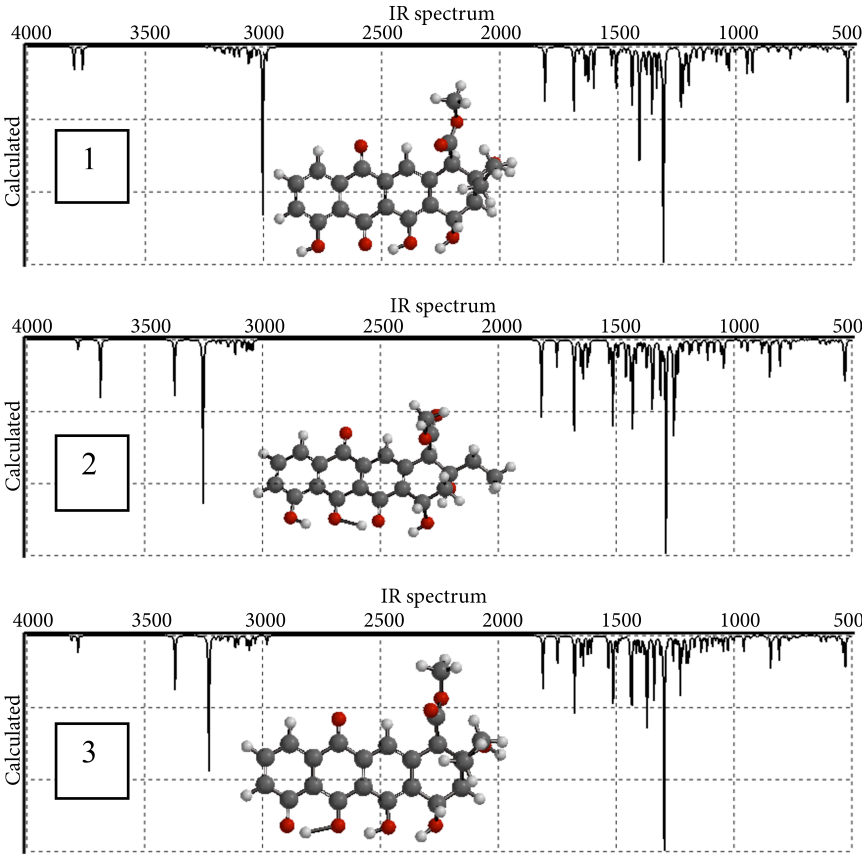

Figure 3. IR spectra of some of the tautomers (RB3LYP/6-31G(d,p)).

course in the realm of DFT. It should be mentioned that the literature on the early work in the field referred to some problems in interpreting Kohn–Sham orbitals of DFT. However, later on it was demonstrated that Kohn–Sham orbitals are compatible with Hartree–Fock (HF) orbitals.[24] In reality, the shapes of Kohn–Sham orbitals seem to be similar to those of canonical HF molecular orbitals. However, it is noteworthy that HF virtual orbitals such as the LUMO tend to be too high in energy and anomalously diffuse compared to Kohn–Sham virtual orbitals. Moreover, it has to be noted that approximate functionals are quite unsatisfactory to predict ionization potentials in this fashion and requires some sort of correction scheme, e.g., an empirical linear scaling of the eigenvalues.[24]

Table 4. The HOMO and LUMO energies (10^{-19} J) and interfrontier energy gaps ($\Delta\varepsilon$) of the structures considered (RB3LYP/6-31G(d,p)).

Structure	HOMO	LUMO	$\Delta\varepsilon$
1	–10.18010124	–4.71053682	5.46956442
2	–10.62049104	–5.1873561	5.43311892
3	–10.50958458	–5.07526416	5.43432042

The patterns of the HOMO and LUMO (RB3LYP/6-31G(d,p)) of some of the tautomers are shown in Figure 4. Note that **2** and **1** are the most stable tautomers in vacuum and in aqueous solution, respectively.

All the tautomers obviously have the same number of heteroatoms; thus the effect of heteroatoms on the

frontier molecular orbitals (FMO, the HOMO and LUMO) energies up to a first approximation should be the same. Moreover, they have the same functional groups in the same number. Therefore, the variations in FMO energies in tautomers **1**–**3** are related to the fine topology of the structures but not their gross topology.

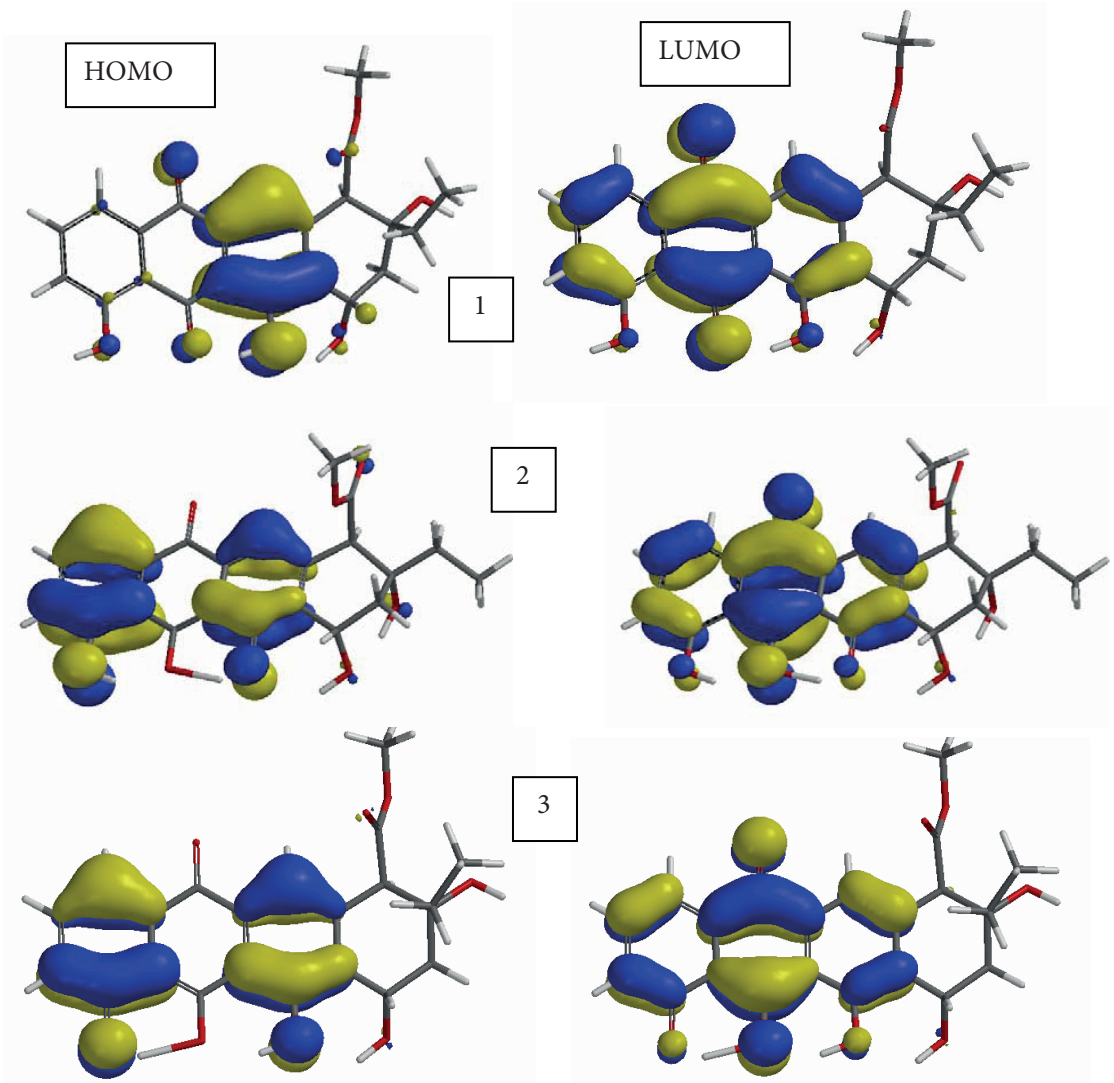

Figure 4. The HOMO and LUMO patterns of some of the tautomers (RB3LYP/6-31G(d,p)).

As seen in Figure 4, the HOMO and LUMO of the tautomers exhibit π-symmetry and it is clearly seen that they are mainly constructed by the contribution of atomic orbitals of the part originating from the anthraquinone moiety.

2.4. Some properties of the charged forms

Since the calculations indicate that in aqueous solution tautomer **1** is more stable than the others, it is worth investigating some properties of anions (phenolates) **1a** and **1c**, where **a** and **c** stand for the phenolic rings of **1** from left to right (see Figures 1 and 5). Table 5 shows the total energies of the phenolate ions originating from **1.** As seen there, both in vacuum and aqueous conditions, **1a** is more stable than **1c**. Table 6 shows

the HOMO and LUMO energies and $\Delta\varepsilon$ values (DFT treatment) of the anions considered. The HOMO and LUMO energies of **1a** are lower than those of **1c.** However, $\Delta\varepsilon$ values are quite comparable.

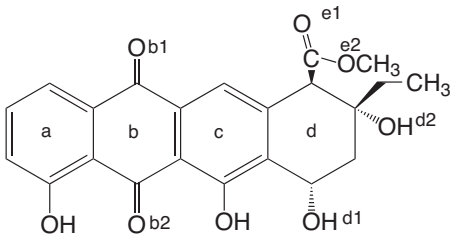

Figure 5. Labeling of the positions for protonation.

Table 5. Energies (kJ) of the phenolate ions of tautomer **1** (RB3LYP/6-31G(d,p)).

Anions	Total energy (vacuum)	Corrected total energy (vacuum)	Corrected total energy (aqueous)
1a	–3,811,470.99	–3,810,485.37	–3,810,863.44
1c	–3,811,406.40	–3,810,417.89	–3,810,729.01

See Figure 5 for the labeling of positions.

Table 6. The HOMO and LUMO energies (10^{-19} J) and interfrontier energy gaps ($\Delta\varepsilon$) of anions of tautomer **1** (RB3LYP/6-31G(d,p)).

Anions	HOMO	LUMO	$\Delta\varepsilon$
1a	–2.78730378	1.0186317	3.80593548
1c	–2.52728316	1.2981006	3.82538376

See Figure 5 for the labeling of positions.

Figure 5 shows the labeling of positions of **1** for protonation. Note that rings **a** and **c** have only one site for protonation, that is the phenolic oxygen atom. Table 7 shows the stabilities of the mono protonated forms of tautomer **1**. The order of stabilities for the protonated species (labeled as the label of the protonated site) in vacuum is **1c** < **1d1** < **1b2** < **1a** < **1b1** < **1e1** < **1e2** < **1d2**, whereas in water it is **1d2** < **1e2** < **1c** < **1e1** < **1d1** < **1b1** < **1b2** < **1a**. The stabilities in vacuum and water conditions are quite different. Note that the most stable cation in the vacuum is **1c**, which is the phenolic oxygen, whereas **1d2** (favored in aqueous conditions) is an alcoholic site.

Table 7. Total energies (kJ) of various protonated forms of tautomer **1** (RB3LYP/6-31G(d,p)).

Cation	Total energy (vacuum)	Corrected total energy (vacuum)	Total energy (aqueous)	Corrected total energy (aqueous)
1a	–3,813,844.20	–3,812,786.38	–3,814,037.70	–3,812,980.14
1b1	–3,813,819.26	–3,812,763.01	–3,814,060.54	–3,813,004.30
1b2	–3,813,876.23	–3,812,815.78	–3,814,057.92	–3,812,997.47
1c	–3,813,898.55	–3,812,839.15	–3,814,270.06	–3,813,210.66
1d1	–3,813,888.84	–3,812,828.91	–3,814,069.21	–3,813,009.28
1d2	–3,813,788.54	–3,812,733.34	–3,814,480.37	–3,813,425.43
1e1	–3,813,804.29	–3,812,748.31	–3,814,174.76	–3,813,118.77
1e2	–3,813,788.80	–3,812,733.60	–3,814,479.84	–3,813,424.64

See Figure 5 for the labeling of positions.

Table 8 includes the HOMO and LUMO energies and the interfrontier energy gaps for the protonated species of tautomer **1**. The protonation lowers both the HOMO and LUMO energies of **1** (see Table 4) drastically. Since unequal lowering in the HOMO and LUMO energies occurs, $\Delta\varepsilon$ values of the protonated species range between 5.57496 $\times$ 10^{-19} J and 3.78072 $\times$ 10^{-19} J. Note that $\Delta\varepsilon$ of unprotonated **1** is 5.46282 $\times$ 10^{-19} J.

Table 8. The HOMO and LUMO energies (10^{-19} J) and interfrontier energy gaps ($\Delta\varepsilon$) of protonated forms of tautomer **1** (RB3LYP/6-31G(d,p)).

Cation	HOMO	LUMO	$\Delta\varepsilon$
1a	–15.4186092	–11.41591608	4.0026771
1b1	–15.5620683	–11.77727922	3.7848051
1b2	–15.40912536	–10.6866216	4.72250376
1c	–15.61147398	–10.55391192	5.05756206
1d1	–15.75986724	–10.69285338	5.06702988
1d2	–13.98172734	–8.41319136	5.56851996
1e1	–14.51288646	–9.23045166	5.28241878
1e2	–13.98034962	–8.41221414	5.56813548

See Figure 5 for the labeling of positions.

3. Conclusion

Among the other tautomeric forms of aklavinone presently concerned, tautomer **2** emerges as the most favorable one, in terms of the free energy of formation from its elements. It is also the most stable one in vacuum conditions in terms of total energy. In aqueous medium, tautomer **1** precedes **2** in stability. However, energetically the tautomers seem not very different from each other. Based on the Gibbs free energy change and within the constraints of the DFT approach employed presently, tautomer **1** appears to turn more favorably into **3** rather than **2**. At this point, kinetic factors should play an important role. As for the phenolate ions obtained from **1,** they show parallelism in stability in vacuum as well as in water. The protonated forms of tautomer **1** exhibit very different stability orders in vacuum and aqueous conditions.

4. Experimental

Presently a routine procedure has been adopted and the initial geometry optimizations of all the structures leading to energy minima were achieved by using the first MM2 (molecular mechanics) method followed by the semiempirical PM3 self-consistent fields molecular orbital (SCF MO) method at the restricted level.[25–27] Then the geometry optimizations were achieved by using various restricted Hartree–Fock (RHF) methods successively. The last stages of optimization were within the framework of DFT (RB3LYP) at the levels of RB3LYP/6-31G(d) and RB3LYP/6-31G(d,p).[28,29] Note that RB3LYP/6-31G(d) and RB3LYP/6-31G(d,p) type calculations produce good results for many purposes, including thermochemistry, the ground state and transition state geometries, etc.[30,31] The exchange term of B3LYP consists of hybrid Hartree–Fock and local spin density (LSD) exchange functions with Becke's gradient correlation to LSD exchange.[32] The correlation term of B3LYP consists of the Vosko, Wilk, Nusair (VWN3) local correlation functional and Lee, Yang, Parr (LYP) correlation correction functional.[33,34]

For each set of calculations, vibrational analyses were also done (using the same basis set employed in the corresponding geometry optimizations). All the results indicated that the normal mode analysis for each structure yielded no imaginary frequencies for the $3N-6$ vibrational degrees of freedom, where N is the number

of atoms in the system. This shows that the structure of each molecule corresponds to at least a local minimum on the potential energy surface. The corrected total energies were obtained by adding zero point vibrational energies (ZPVE) to uncorrected total energy values. All these computations were performed by using the Spartan 06 package program.[35]

References

1. Clark, B.; Capon, R. J.; Stewart, M.; Lacey, E.; Tennant, S.; Gill, J. H. *J. Nat. Prod.* **2004**, *67*, 1729–1731.
2. Marco, A. D.; Gaetani, M.; Orrezi, P.; Scarpinato, B. M.; Silvestrini, R.; Soldati, M.; Dastia, T.; Valentini, L. *Nature* **1964**, *201*, 706–707.
3. Dharmaraj, S. *World J. Microbiol. Biotechnol.* **2010**, *26*, 2123–2139.
4. Hauser, F. M.; Mal, D. *J. Am. Chem. Soc.* **1984**, *106*, 1098–1104.
5. Arcamone, F. *Doxorubicin: Anticancer Antibiotics*, Academic Press, New York, 1981.
6. Oki, T.; Matsuzawa, Y.; Yoshimoto, A.; Numata, K.; Kitamura, I.; Hori, S.; Takamatsu, A.; Umezawa, H.; Ishizukia, M.; Naganawa, H.; Suda, H.; Hamada, M.; Takeuchi, T. *J. Antibiot.* **1975**, *28*, 830–834.
7. Oki**,** T.; Kitamura, I.; Yoshimoto, A.; Matsuzawa, Y.; Shibamoto, N.; Ogassawara, T.; Inui, T.; Takamatsu, A.; Takeuchi, T.; Masuda, T.; Hamada, S.; Suda**,** J.; Ishizuka, M.; Sawa, T.; Umezawa, H. *J. Antibiot.* **1979**, *32*, 791–800.
8. Oki, T.; Shibamoto, N.; Matsuzawa, Y.; Ogasawara, T.; Yoshimoto, A.; Kitamura, I.; Inui, T.; Naganawa, H.; Takeuchi, T.; Umezawa, H. *J. Antibiot.* **1977**, *30*, 683–687.
9. Yamaki, H.; Suzuki, H.; Mishimura,T.; Tanaka, N. *J. Antibiot.* **1978**, *31*, 1149–1154.
10. Taneka, H.; Yoshioka, T.; Shimauchi, Y.; Matsuzawa, Y.; Oki, T.; Inui, T. *J. Antibiot.* **1980,** *33*, 1323–1330.
11. Kerde, A. S.; Rizzi, J. P. *J. Am. Chem. Soc.* **1981**, *103*, 4247–4248.
12. Pearlman, B. A.; McNamara J. M.; Hasan, I.; Hatakeyama, S.; Sekizaki, H.; Kishi, Y. *J. Am. Chem. Soc.* **1981**, *103*, 4248–4251.
13. Confalone, P. N.; Pizzalato, G. *J. Am. Chem. Soc.* **1981**, *103*, 4251–4254.
14. Li, T.; Wu, Y. L. *J. Am. Chem. Soc.* **1981**, *103*, 7007–7009.
15. Jones, D. W.; Lock, C. J. *J. Chem. Soc. Perkin Trans.* 1 **1995**, 2747–2755.
16. Kleyer, D. L.; Koch, T. H. *J. Am. Chem. Soc.* **1984**, *106*, 2380–2387.
17. Kodama, M.; Misako, A.; Chikayoshi, N.; Toshikazu, O.; Yasue, M. *Cancer Biochemistry Biophysics* **1983**, *6*, 243–247.
18. Solomons, T. W. G.; Fryhle, C. B. *Organic Chemistry*, Wiley, New York, 2004.
19. Kleyer, D. L.; Guardino, G.; Koch, T. H. *J. Am. Chem. Soc.* **1984**, *106*, 1105–1109.
20. Türker, L. *The Scientific World Journal*, **2012**, doi: 10.1100/2012/526289.
21. Egorov, N. S. *Antibiotics, A Scientific Approach*, Mir Pub., Moscow, 1985.
22. Reutov, O. *Theoretical Principles of Organic Chemistry*, Mir Pub., Moscow, 1970.
23. Reichardt, C. *Solvents and Solvent Effects in Organic Chemistry*, Wiley-VCH, Weinheim, 2004.
24. Cramer, C. J. *Essentials of Computational Chemistry*, Wiley, Chichester, 2004.
25. Stewart, J. J. P. *J. Comput. Chem.* **1989**, *10*, 209–220.
26. Stewart, J. J. P. *Appl. J. Comput. Chem.* **1989**, *10*, 221–264.
27. Leach, A. R. *Molecular Modeling*, Longman, Essex, 1997.
28. Kohn, W.; Sham, L. J. *Phys. Rev.* **1965**, *140*, 1133–1138.

29. Parr, R. G.; Yang, W. *Density Functional Theory of Atoms and Molecules*, Oxford University Press, London, 1989.
30. Spartan. *Molecular Modeling in Physical Chemistry*, Wavefunction, Irvine, 2005.
31. Young, D .C. *Computational Chemistry*, Wiley-Interscience, NY, 2001.
32. Becke, A. D. *Phys. Rev.*, A **1988**, *38*, 3098–3100.
33. Vosko, S. H.; Vilk, L.; Nusair, M. *Can. J. Phys.* **1980**, *58*, 1200–1211.
34. Lee, C.; Yang, W.; Parr, R.G. *Phys. Rev.*, B **1988**, *37*, 785–789.
35. SPARTAN 06. Wavefunction Inc., Irvine CA, USA, 2006.